Meso-scale structures and anomalous convective transport at the edge of magnetic confinement devices

Sergei Krasheninnikov

University of California at San Diego, USA

with contributions from

A. I. Smolyakov[1], G. Yu[2], and T. K. Soboleva[3]

[1]*University of Saskatchewan, Saskatoon, Canada*
[2]*University of California at San Diego, La Jolla, CA, USA*
[3]*UNAM, Mexico D.F., Mexico and Kurchatov Institute, Moscow, Russia*

Workshop on New Directions for Advanced Computer Simulations and Experiments in Fusion-Related Plasma-Surface Interactions for Fusion
ORNL, Oak Ridge, TN, March 21-23, 2005

Outline

I. Recent accomplishments

II. Parallel E×B shear drive and plasma radial convection

III. $\nabla_{\perp} T_e$ drive and plasma radial convection

IV. Estimates

V. Conclusions

I. Recent accomplishments

- In many cases strongly localized filaments of plasma pressure inhomogeneities emerge in the tokamaks
- The examples of such cases are the plasma blobs in the scrape of layer (SOL), pellet clouds, ELMs

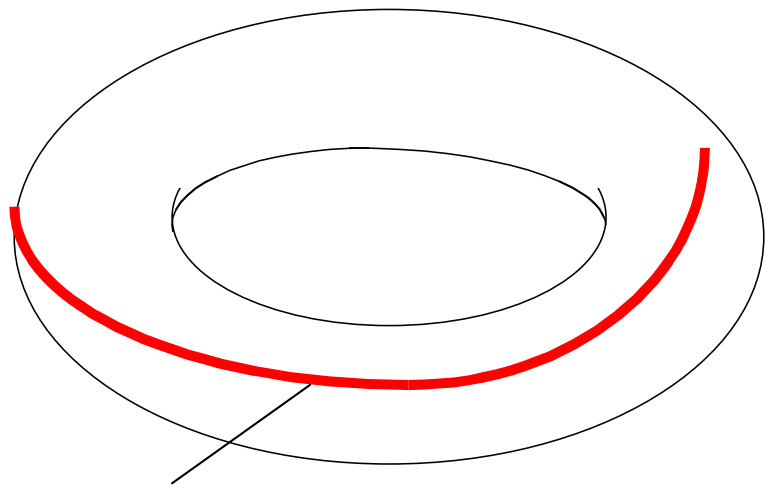

- They all exhibit more convective rather than diffusive radial transport of plasma
- Similar features of convective crossfield plasma transport toward the wall were observed also in stellarators and linear plasma devices
- Rather comprehensive study of these phenomena shows striking similarities between them through different devices

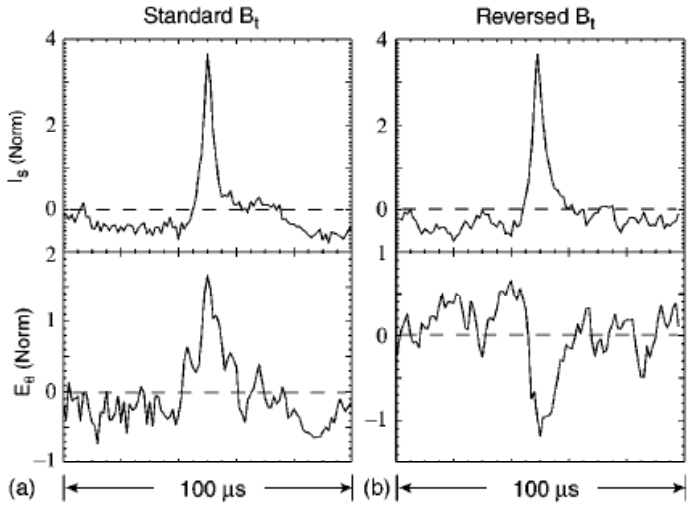

Blobs in DIII-D, Boedo, PoP 2001

Blobs at LAPD, Carter, APS-2002

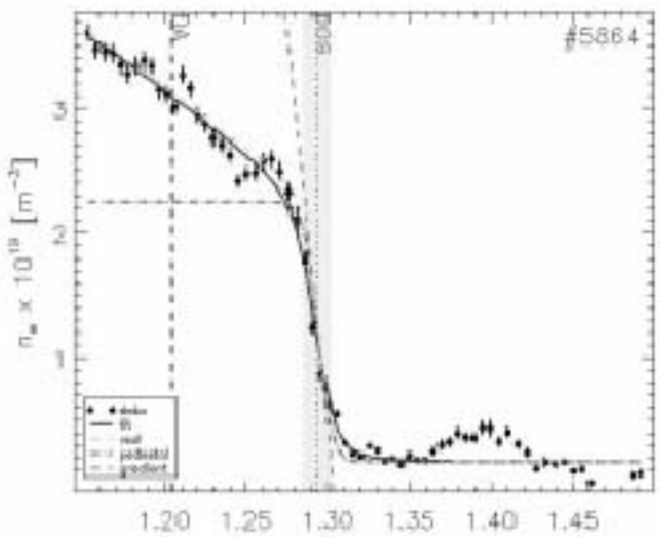

Kirk et al., "**Observations of the structure of ELMs on MAST**"
ST workshop 2003, Culham 15 - 17th September 2003

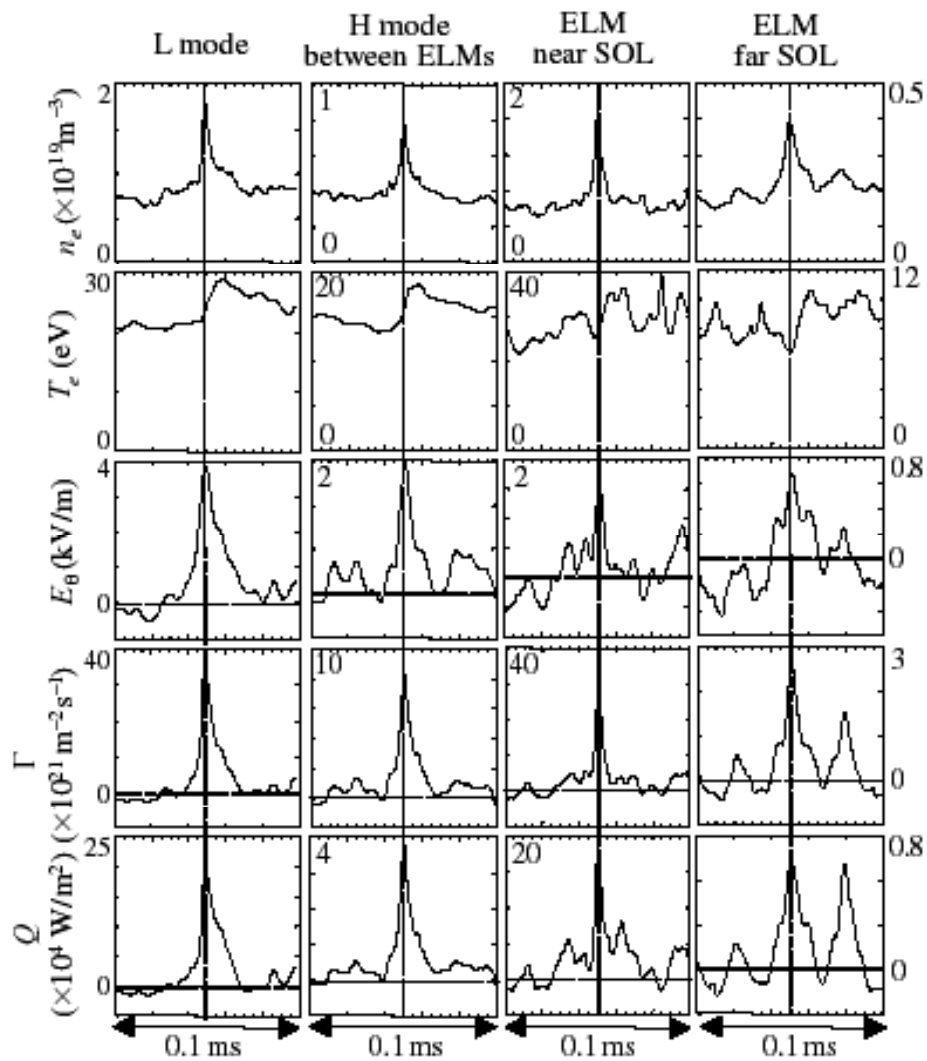

Rudakov, et al., Plasma Phys. Control. Fusion **44** (2002) 717

- The ∇B in toroidal and "neutral wind" in linear devices result in plasma polarization and, correspondingly, the **E**×**B** radial convection of the blobs with radial velocity $V_b \sim 1000\ m/s$ (Krasheninnikov, TTF-1998, PLA, **283** (2001) 368; D'Ippolito et al., PoP **9** (2002) 222; Bian, et al., PoP **10** (2003) 671; Krasheninnikov and Smolyakov, Phys. Plasmas **10** (2003) 3020)

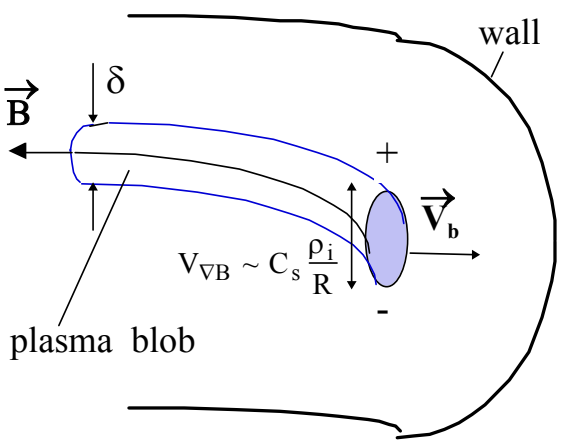

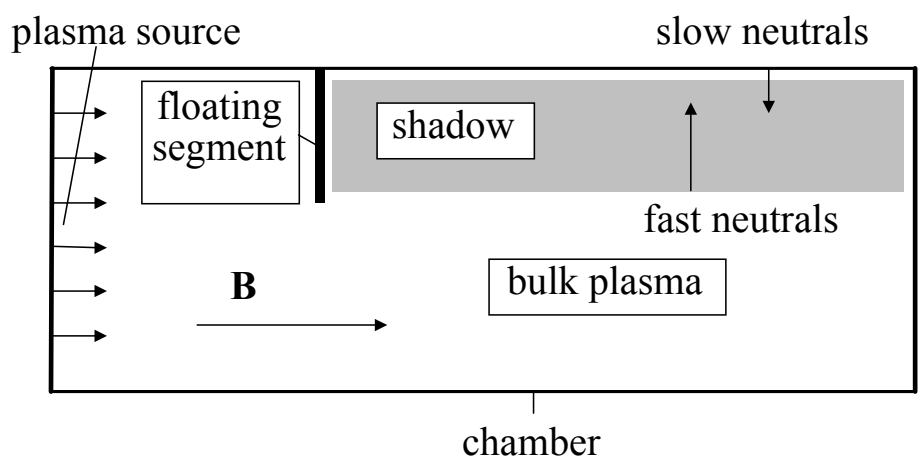

linear device

tokamak

- For $T_e = \text{const.}$ we describe both ∇B and "neutral wind" effects

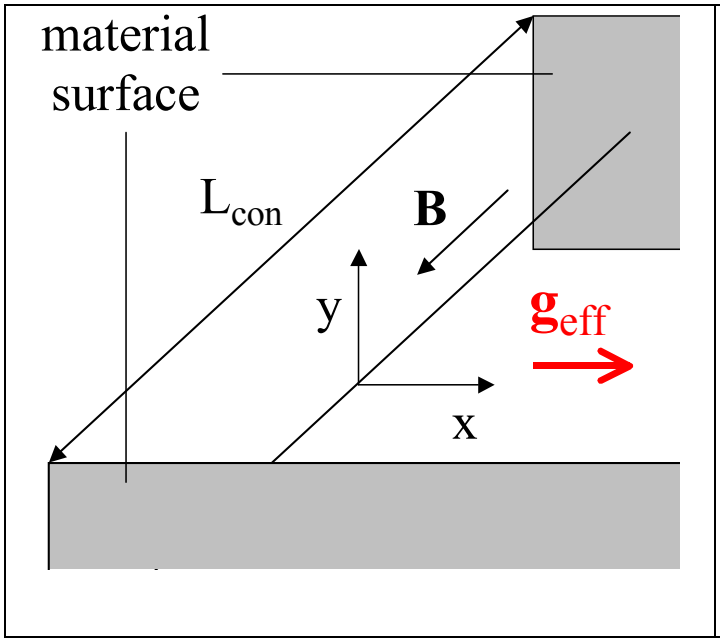

$$\nabla_\perp \cdot (n d_t \nabla_\perp \phi) + C_s \eta \partial_y n =$$

$$= (2C_s / \rho_s^2 L_{con}) n\phi$$

$$d_t n = 0$$

$$d_t(\ldots) = \partial_t(\ldots) + \mathbf{V}_{E\times B} \cdot \nabla(\ldots)$$

$$\eta_{\nabla B} \equiv 2/\rho_s R; \quad \eta_{nw} \equiv \xi_{f/s}(\nu_{iN} / \rho_s^2 \omega_{Bi}); \quad V_b = C_s \eta \left(\rho_s^3 L_{con} / \delta_y^2\right)$$

- 2D numerical modeling suggests that only the blobs with $\delta_b \sim \delta_* \equiv 2\rho_s (L/\rho_s)^{2/5} (\eta)^{1/5}$ seems to be able to move as a coherent structures at large distance

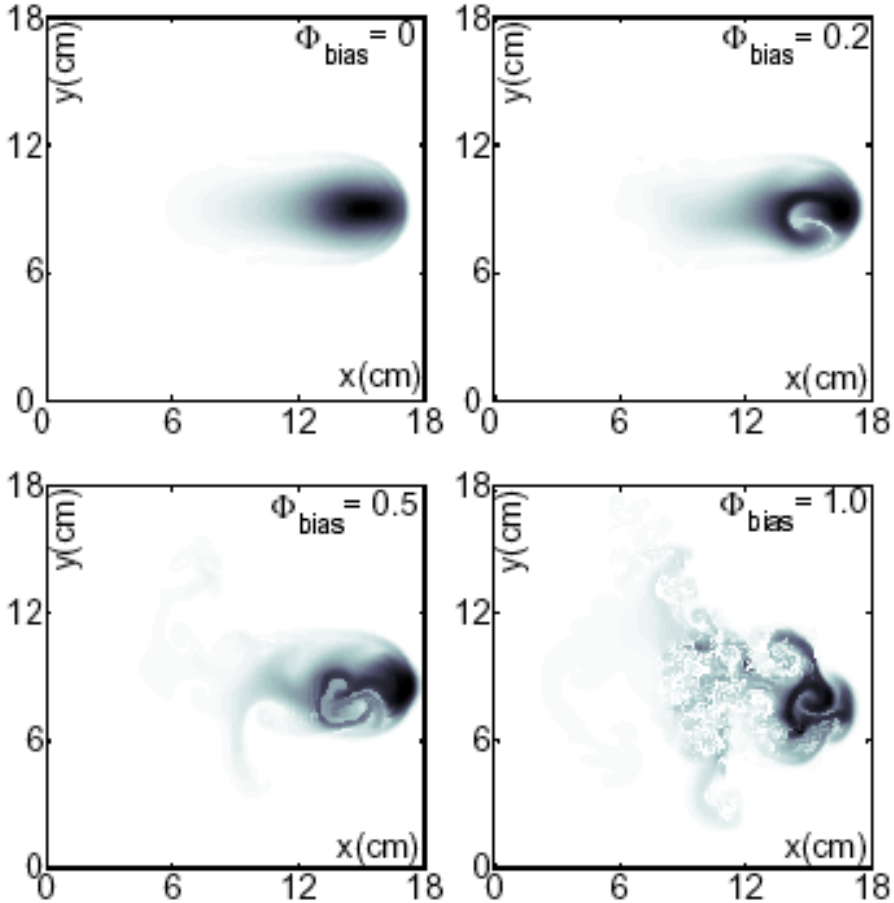

Impact of sheared biasing (Yu and Krasheninnikov PoP, 2003)

Blobs in the vicinity of separatrix, effect of X-point

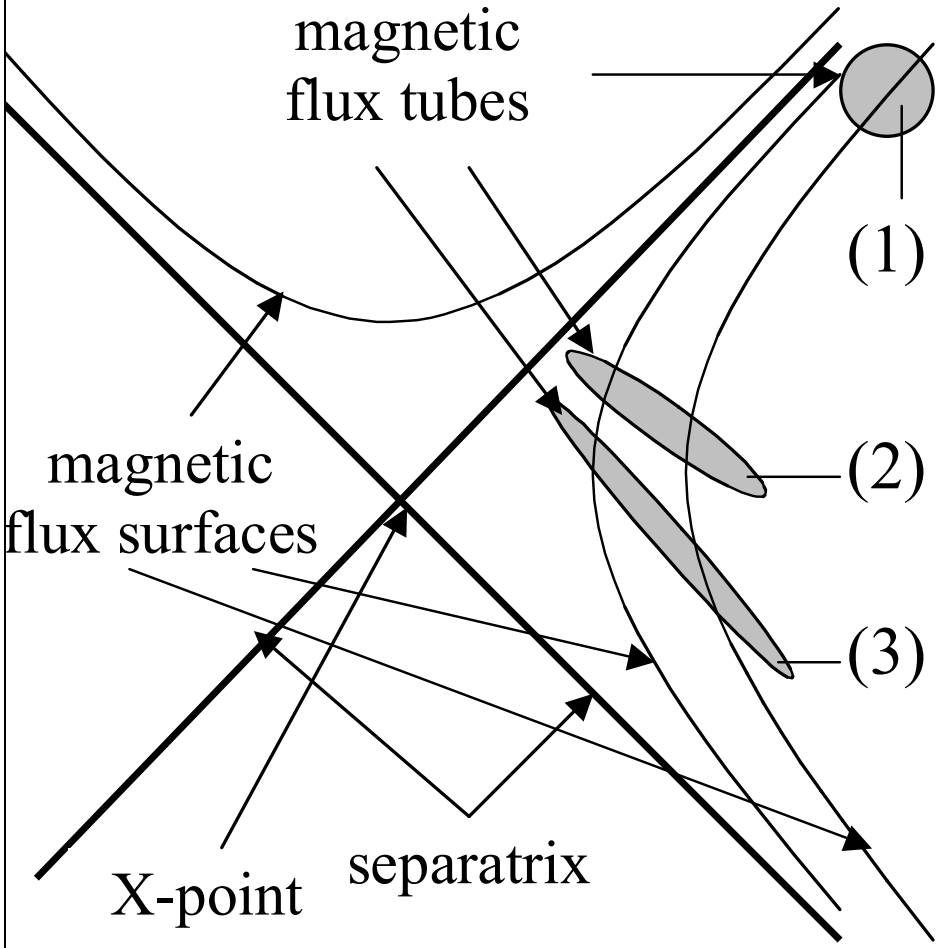

Strong magnetic shear in the vicinity of X-point results in dramatic squeezing of magnetic flux tubes to the level below ion larmor radius (D. Farina, R. Pozzoli, and D. D. Ryutov, Nucl. Fusion **33,** 1315 (1993))

- As a result, plasma cross-field resistivity becomes important
- Introduce squeezing function $S(\ell) \approx \exp(-\ell / L_X)$, where ℓ is the length along the magnetic field line and L_X is the effective squeezing length (in current large tokamaks $L_X \sim 10^3$ cm)
- The effective wave number of the potential perturbation varies as follows: $K(\ell) = k / S(\ell)$, where k is the wave number at the entrance into X-point region
- We balance perpendicular, $j_\perp = -i\sigma_\perp K(\ell)\varphi$, and parallel, $j_{||} = -\sigma_{||}(\partial\varphi / \partial\ell)$, currents and get

$$\partial^2\varphi / \ell^2 = -(\sigma_\perp / \sigma_{||})K^2(\ell)\varphi$$

- As a result we find relations between parallel current and electrostatic potential at the entrance to X-point region

$$j_{\|}\big|_{entr} \approx \sigma_{eff}\,|\,k\,|\,\varphi\big|_{entr}, \qquad \text{where } \sigma_{eff} = \omega_{pe}^2/(4\pi\Omega_e)$$

- Approximating wave number of the blob at the entrance into X-point region as $k \sim 1/\delta_b$, we use this relation in 2D vorticity equation and find

$$\rho_s^2 \nabla_\perp \cdot \left\{ n \frac{d\nabla_\perp \phi}{dt} \right\} + \frac{2\rho_s C_s}{R} \frac{\partial n}{\partial y} = \frac{2C_s}{L_b} \frac{\rho_s}{\delta_b} n\phi \quad \Rightarrow \quad V_b \sim C_s \frac{\rho_s}{\delta_b} \frac{L_b}{R}$$

(Krasheninnikov, Ryutov, and Yu, to appear in the Journal of Plasma and Fusion Research, 2005)

High □ blobs vs pellet clouds and ELMs

- So far we neglect an impact of blob on the structure of the magnetic field assuming that β_b is small

$$\frac{B_r}{B} \sim \frac{4\pi}{c} j_{||}\delta_b \sim \beta_b \frac{L_b}{R}$$

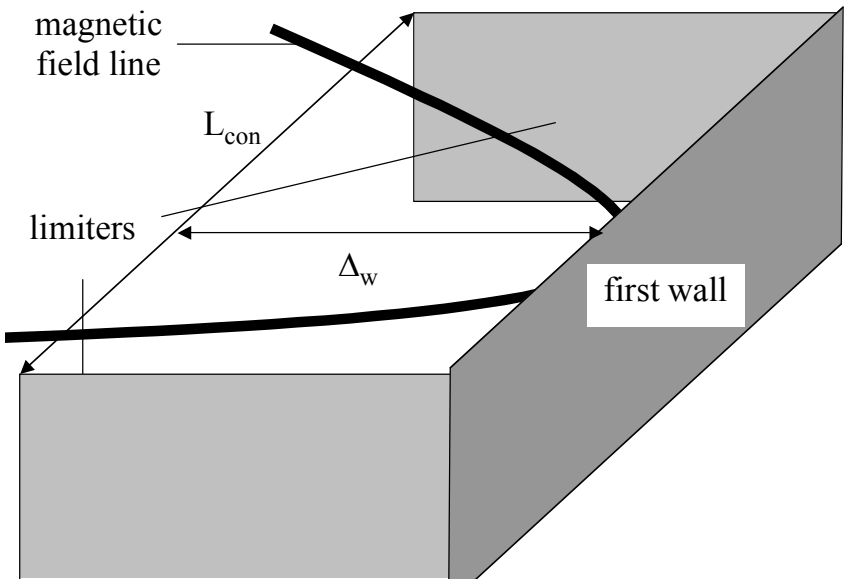

- At relatively large β_b bending of the magnetic field lines become so strong

$$\beta_b \gtrsim \beta_{crit} \sim \frac{R\Delta_w}{L_{con}^2}$$

- To describe the evolution of blobs with $\beta_b > \beta_{crit}$ within the framework of simple 2D model we use the approach adopted for pellet cloud dynamics (V. Rozhansky, et al., Plasma Phys. Control. Fusion **37,** 399 (1995); P. B. Parks, et al., Phys. Plasmas, **7,** 1968 (2000))

- Introducing vector potential $A_{||}$ and using linear relations to account for the bending of magnetic field we find

$$\varphi = \frac{V_A}{c} A_{\parallel} \quad \Rightarrow \quad j_{\parallel} = -\frac{c^2}{4\pi V_A} \nabla_{\perp}^2 \varphi$$

$$\rho_s \nabla_{\perp} \cdot \left\{ n \frac{d\nabla_{\perp}\phi}{dt} \right\} + \frac{2C_s}{R} \frac{\partial n}{\partial y} = -\frac{2V_A}{L_b} n_{amb} \rho_s \nabla_{\perp}^2 \phi$$

- We find that "blob" velocity is independent on δ_b

$$V_b \sim C_s \frac{C_s}{V_A} \frac{L_b}{R} = C_s \sqrt{\beta} \frac{L_b}{R} \sim 0.1 \times C_s$$

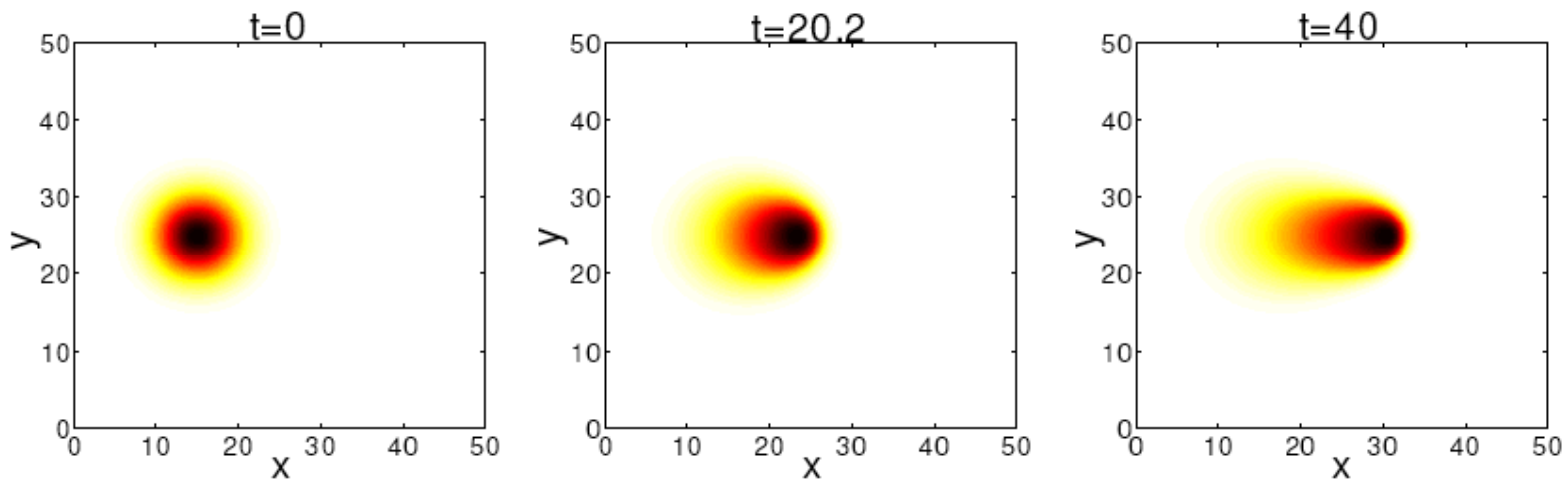

Pelets/ELMs/high □ blobs

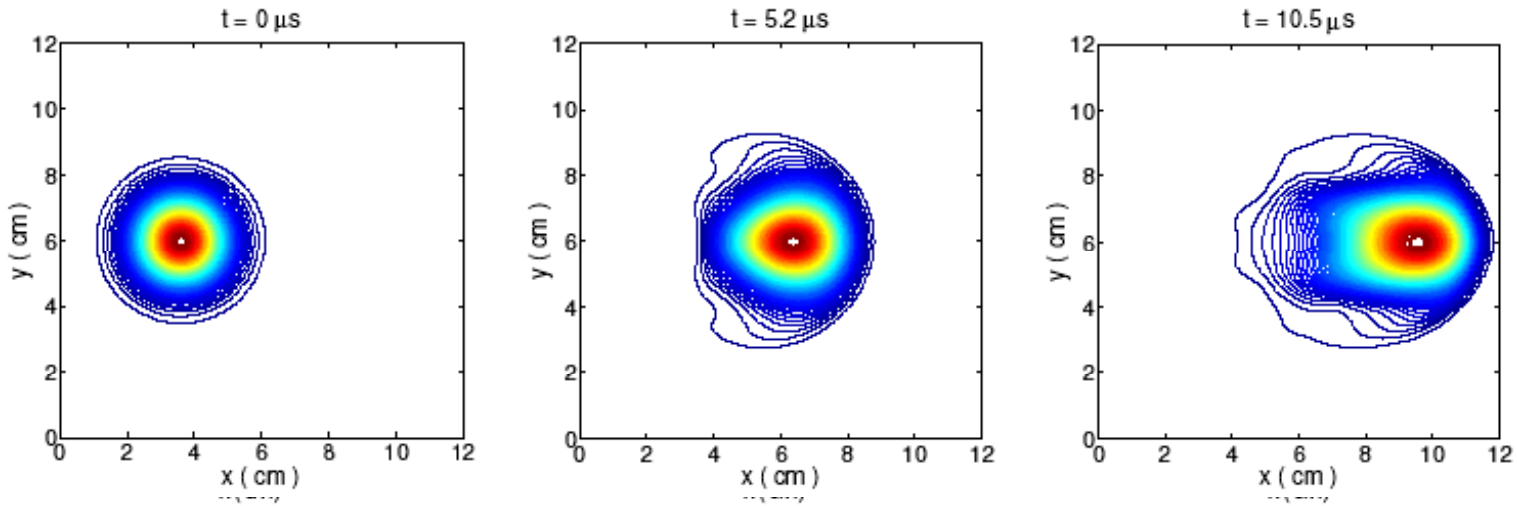

“Sheath” blobs

II. Parallel E×B shear drive and plasma radial convection

- The drive responsible for the parallel **E×B** shear instability (Kadomtsev 1965, Lee, Catto, Aamodt, 1982; Tsidulko, Berk, Cohen, 1994; Myra, D'Ippolito, Goedbloed, 1997) can result in convective transport

- For $T_e = \text{const.}$ we use electron parallel momentum balance equation, $\nabla \cdot \mathbf{j} = 0$, and continuity equation

$$\frac{1}{c}\frac{\partial \psi}{\partial t} + \nabla_{||}\left(\frac{T_e}{e}\ln(n) - \varphi\right) = 0, \quad \nabla_{\perp} \cdot \left(\frac{c}{V_A^2}\frac{d}{dt}\nabla_{\perp}\varphi\right) = \nabla_{||}\nabla_{\perp}^2\psi, \quad \frac{d}{dt}n = 0$$

- Introducing $G = \phi - \ln(n/n_{\infty})$, from these equations we have

$$\frac{\partial}{\partial t}\nabla_\perp \cdot \left(\frac{1}{V_A^2}\frac{d}{dt}\nabla_\perp \phi\right) = \nabla_\parallel^2 \nabla_\perp^2 G, \qquad \frac{\partial}{\partial t}\phi = \frac{d}{dt}G. \qquad (1)$$

- Introducing $G = \phi - \Lambda$ and neglecting nonlinearities in LHS of (1) outside blob we find

$$\frac{1}{V_{A_\infty}^2}\frac{\partial^2}{\partial t^2}G = \nabla_\parallel^2 G \Rightarrow G = G_{(+)}(\ell_\parallel - V_{A_\infty} t),\ G = G_{(-)}(\ell_\parallel + V_{A_\infty} t) \quad (2)$$

- Integrating (1) over blob in $\parallel$ coordinate and using (2) we find

$$L_b \frac{\partial}{\partial t}\nabla_\perp \cdot \left(\frac{1}{V_A^2}\frac{d}{dt}\nabla_\perp \phi\right) = \frac{\partial}{\partial \ell_\parallel}\nabla_\perp^2 G\Big|_{-\text{blob}}^{+\text{blob}} = -\frac{2}{V_{A_\infty}}\frac{\partial}{\partial t}\nabla_\perp^2 G \qquad (3)$$

- From Eq. (1) and (3) we have

$$\frac{L_b V_{A_\infty}}{2V_A^2}\frac{d}{dt}\nabla_\perp\phi = -\nabla_\perp G; \qquad \frac{\partial}{\partial t}\phi = \frac{d}{dt}G \tag{4}$$

- In a long wavelength approximation, $\partial_t(...) << \mathbf{V}_E \cdot \nabla(...)$, from (4) we find

$$\boxed{\frac{\partial}{\partial t}\phi = -\frac{L_b V_{A_\infty}}{2V_A^2}\mathbf{V}_E \cdot \{(\mathbf{V}_E \cdot \nabla_\perp)\nabla_\perp\phi\} \tag{5}}$$

- From (5) we recover Lee, Catto, Aamodt: $\gamma = (L_b / 2V_A)(\mathbf{V}_E \cdot \mathbf{k})^2$

- We are looking for solution of (5) in the form of traveling wedge

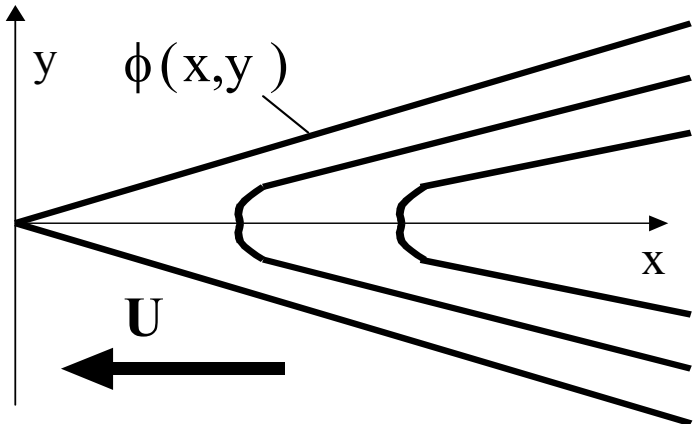

$$\eta = y/(x+Ut)^{\beta} \quad (6); \qquad \phi(x,y,t) = (x+Ut)^{\alpha} F\left(y/(x+Ut)^{\beta}\right), \quad (7)$$

- For $V_{A_\infty} \approx V_A$ substituting (7) into (5) we find: $\beta = \alpha - 1/2$ and

$$u\left(\alpha F - (\alpha - 1/2)\eta \frac{dF}{d\eta}\right) = -\alpha^2 F^2 \frac{d^2F}{d\eta^2} + \left(\frac{dF}{d\eta}\right)^2 \left\{\alpha(2-\alpha)F - (\alpha - 1/2)(3/2 - \alpha)\eta \frac{dF}{d\eta}\right\} \quad (8)$$

where $u = 2V_A U / L_b (C_s \rho_s)^2$

- We solve Eq. (8) numerically for $\alpha = 3/2$, here $F(\eta) \propto (\eta_0 - \eta)^{1/2}$ at $\eta = \eta_0$, and $F(\eta > \eta_0) = 0$ can be matched by diffusion

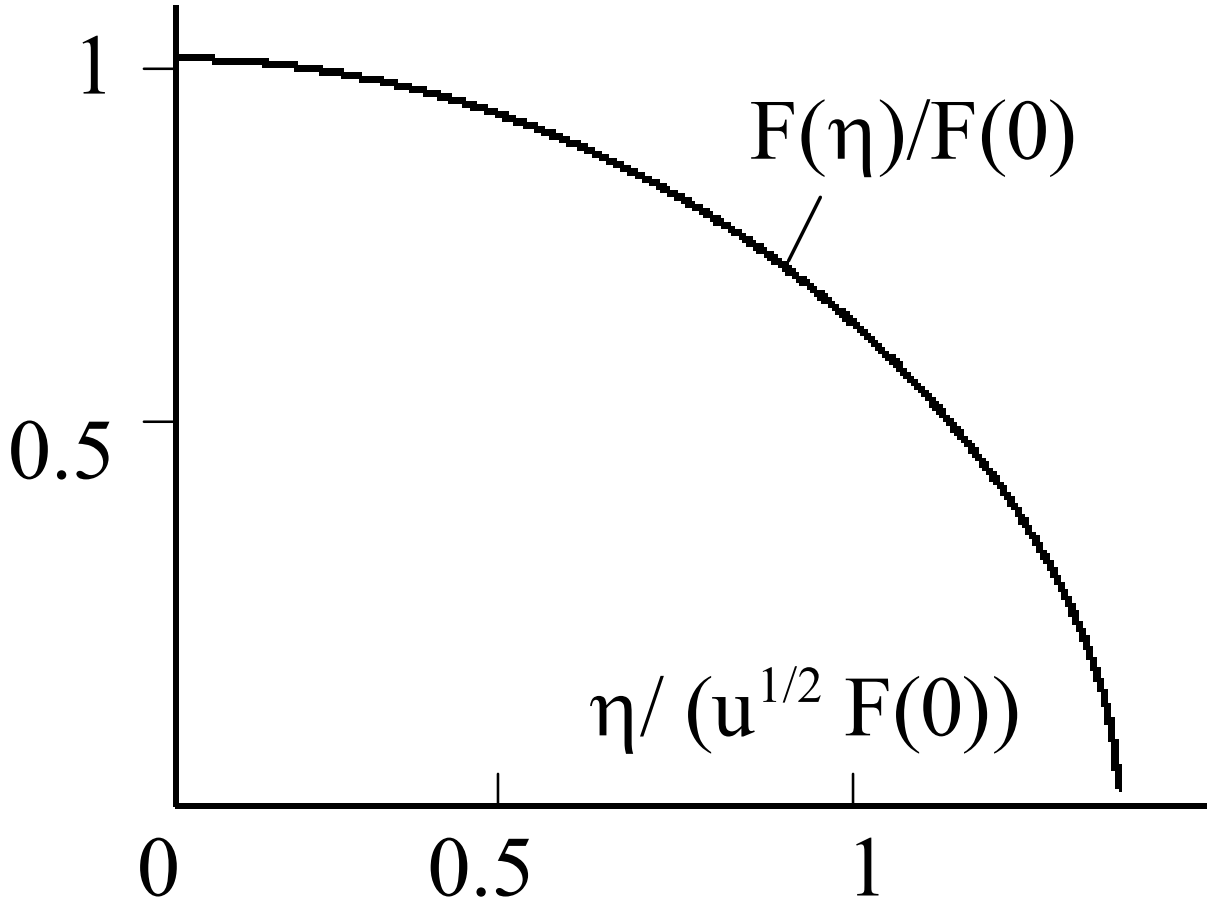

- From here we find $U \approx U_{\|} \equiv C_s \frac{L_b C_s}{\rho_s V_A} \frac{(\phi_0(x))^2 \rho_s^3}{(y_0(x))^3}$; $\phi_0(x)$ and $y_0(x)$ are the normalized potential and wedge's width

III. $\nabla_\perp T_e$ drive and plasma radial convection

- The drive responsible for $\nabla_\perp T_e$ instability in SOL (H. L. Berk, D. D. Ryutov, and Yu. A. Tsidulko, 1991; H. L. Berk, R. H. Cohen, D. D. Ryutov, *et al*., 1993; X. Q. Xu, M. N. Rosenbluth, and P. H. Dimond, 1993; Myra, D'Ippolito, Goedbloed, 1997; D. D. Ryutov and R. H. Cohen, Contr, 2004) can also result in convective transport

- This instability is associated with the effective sheath resistivity which relates plasma current through the sheath, j_{sh}, and electrostatic potential φ relative to the wall

$$j_{sh} = en_{sh}\sqrt{\frac{T_e}{M}}\left\{1-\sqrt{\frac{M}{2\pi m}}\exp\left(-\frac{e\varphi}{T_e}\right)\right\}, \qquad (9)$$

- Assuming that plasma density, temperature, and electrostatic potential are uniform along the field lines, we vorticity equation integrate plate to plate and use (9) as a boundary condition for $j_{||}$:

$$\nabla_{\perp}\cdot\left(\frac{n}{M\Omega_i^2}\frac{d}{dt}\nabla_{\perp}(e\varphi)\right)=\frac{2n}{L_{con}}\sqrt{\frac{T_e}{M}}\left\{1-\sqrt{\frac{M}{2\pi m}}\exp\left(-\frac{e\varphi}{T_e}\right)\right\}, \quad (10)$$

where L_{con} is the connection length

- In addition to Eq. (10) we use energy balance equation in simplest form of advection of electron temperature

$$\frac{d}{dt}T_e=0. \quad (11)$$

- Although the plasma contact with end plate is crucially important for Eq. (10), it can be neglected in electron temperature equation

- To simplify the problem even more we assume constant plasma density and relatively small variation of plasma temperature potential $T_e = T_0 + \delta T_e$, $\varphi = \varphi_0 + \delta\varphi$, where $|\delta T_e| < T_0 = \text{const.}$ and $|\delta\varphi| < \varphi_0 = \text{const.}$

- Then from Eq. (10) and (11) we have

$$\frac{\rho_s^2 L_{con}}{2C_s}\frac{d}{dt}\nabla_\perp^2\phi = \phi - \vartheta, \qquad \frac{d}{dt}\vartheta = 0. \qquad (12)$$

where $\phi = e\delta\varphi / T_0$ and $\vartheta = 0.5\ln(M/2\pi m)\delta T_e$

- In a long wavelength approximation, $\partial_t(...) << \mathbf{V}_E \cdot \nabla(...)$, we find

$$\frac{2C_s}{\rho_s^2 L_{con}} \frac{\partial \phi}{\partial t} = \mathbf{V}_E \cdot \nabla \left\{ \mathbf{V}_E \cdot \nabla \left(\nabla_\perp^2 \phi \right) \right\} \tag{13}$$

- From (13) we recover the result of Berk, Ryutov, and Tsidulko:

$$\gamma = \left(\rho_s^2 L_{con} / 2C_s \right) (\mathbf{V}_E \cdot \mathbf{k})^2 k^2$$

- Introducing $w = 2U/(\rho_s^4 L_{con} C_s)$ and applying ansatz (7) to Eq. (13) we find $\beta = 1$, $\alpha = 5/2$, and, for $\partial_y(...) << \partial_x(...)$,

$$w\left(\frac{5}{2} F - \eta \frac{dF}{d\eta} \right) = \frac{d^2F}{d\eta^2}\left(\frac{dF}{d\eta}\right)^2 - \frac{5}{2} F \left(\frac{d^2F}{d\eta^2} \right)^2 + 5F \frac{dF}{d\eta} \frac{d^3F}{d\eta^3} + \frac{25}{2} F^2 \frac{d^4F}{d\eta^4} \tag{14}$$

- We solve (14) numerically searching for the solution, which approaches zero at $\eta = \eta_0$ as $F(\eta) \propto (\eta_0 - \eta)^{3/2}$, and which can be matched with unperturbed solution $\delta\varphi = 0$ outside the wedge

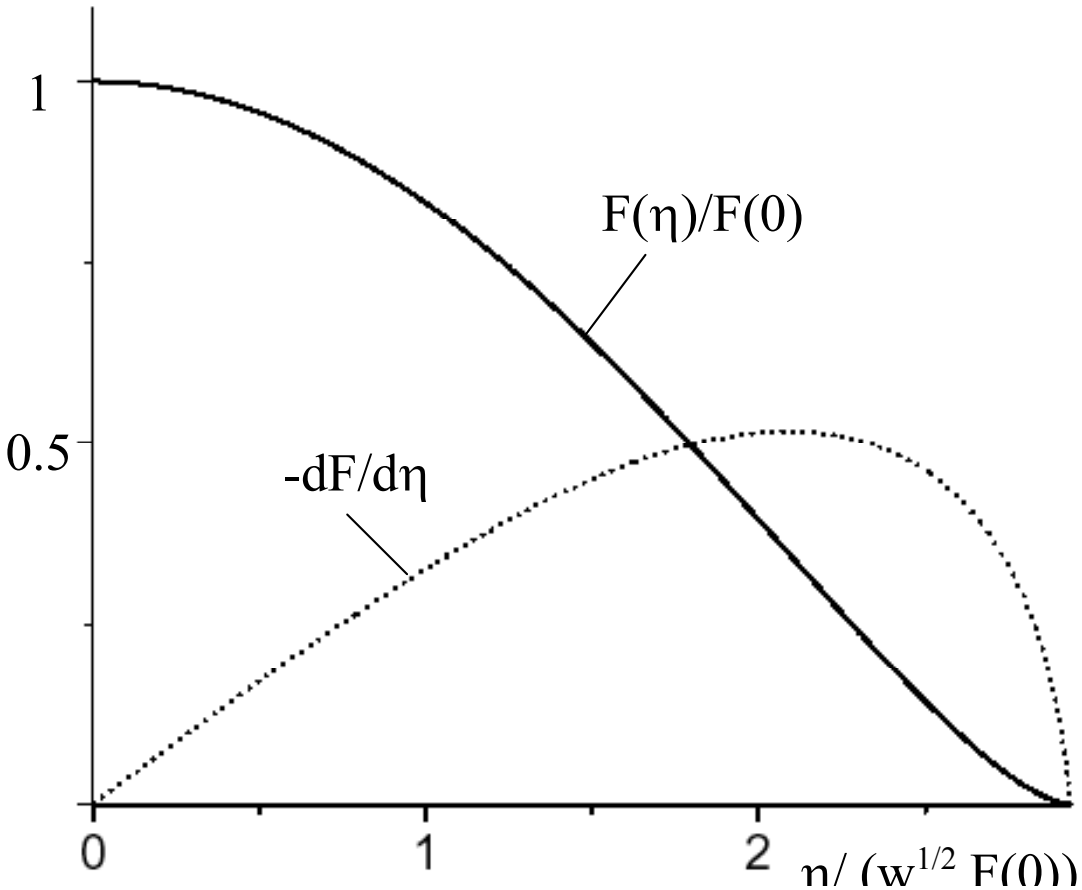

- As a result we get the following expression for convective velocity $U \approx U_{\nabla T_e} \equiv 45 C_s (\phi_0(x))^2 \eta_0 \dfrac{\rho_s^4 L_{con}}{(y_0(x))^5}$

- Numerical simulation also shows that the wedge-like structures are formed and convected radially

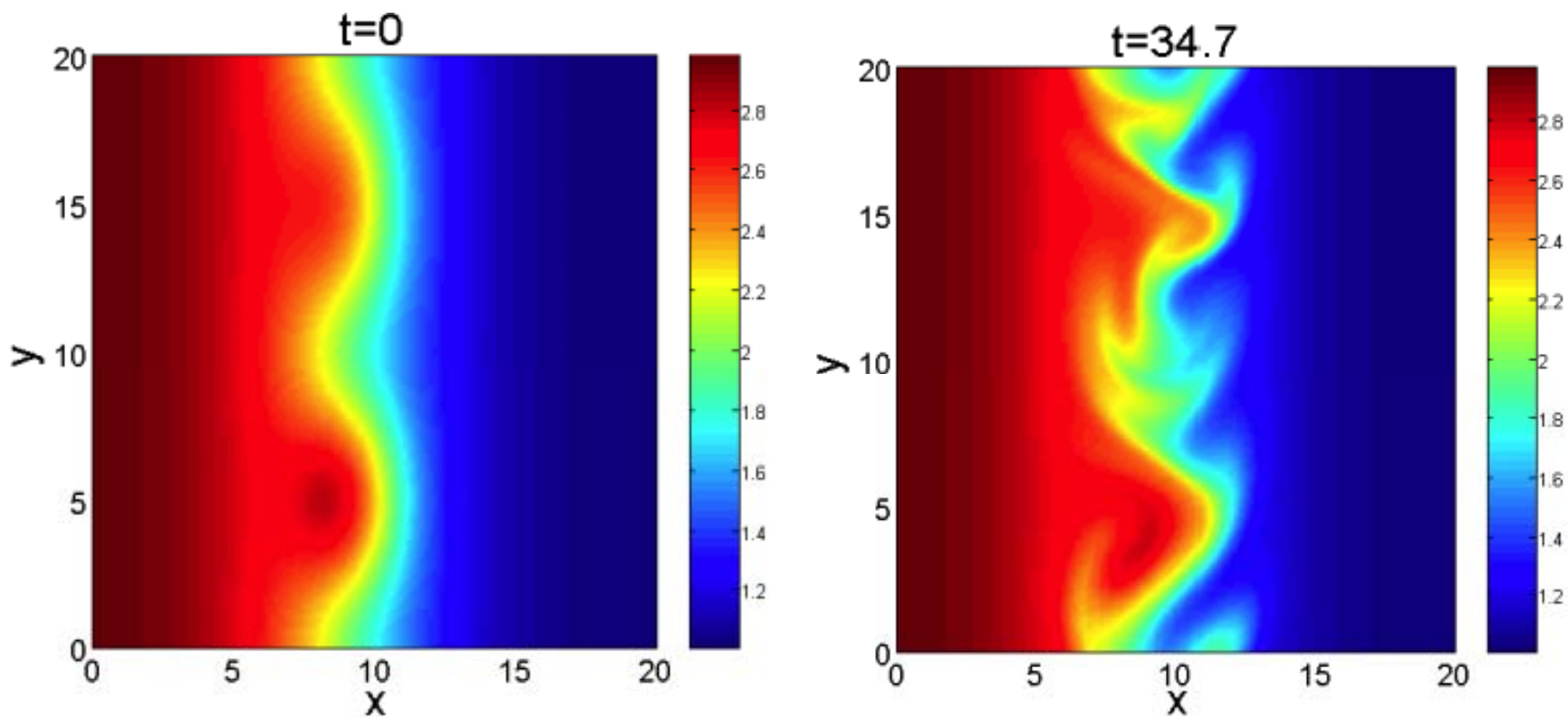

- However, more modeling is needed to verity the analytic results and describe the process of the formation of coherent structures

IV. Estimates

- Estimating $\mathbf{V}_E \cdot \nabla(...) \sim C_s \phi_0(x) \rho_s / y_0^2(x)$ and $\partial_t(...) \sim u / y_0(x)$ we find both $\delta_{(...)} \sim k_*^{-1}$ and $U_{||}(\delta_{||})$ and $U_{\nabla T_e}(\delta_{\nabla T_e})$

$$\boxed{\begin{aligned} \frac{\delta_{||}}{\rho_s} &\approx \left(\frac{L_b}{\rho_s}\beta_p^{1/2}\right)^{1/2}, \qquad \frac{U_{||}(\delta_{||})}{C_s} \approx \left(\beta_p^{-1/2}\frac{\rho_s}{L_b}\right)^{1/2} \\ \frac{\delta_{\nabla T_e}}{\rho_s} &\approx \left(\frac{L_{con}}{\rho_s}\right)^{1/4}, \qquad \frac{U_{\nabla T_e}(\delta_{\nabla T_e})}{C_s} \approx \left(\frac{\rho_s}{L_{con}}\right)^{1/4}, \end{aligned}} \qquad (15)$$

- For $\beta_p \sim 10^{-3}$, and $L_b / \rho_s \sim L_{con} / \rho_s \sim 3 \times 10^4 \Rightarrow$

$$\rho_s/\delta_{||} \sim (U_{||})_\delta / C_s \sim 0.03 \text{ and } \rho_s/\delta_{\nabla T_e} \sim \left(U_{\nabla T_e}\right)_\delta / C_s \sim 0.1,$$

which is consistent with experimental observations

V. Conclusions

- We find that blob dynamics in tokamk and linear devices can be described with some particular class of equations which explain similarity in experimental data from these machines

$$\rho_s^2 \nabla_\perp \cdot \left\{ n \frac{d\nabla_\perp \phi}{dt} \right\} + C_s \eta \frac{\partial n}{\partial y} = \frac{2C_s}{L_{con}} n\phi \qquad \text{(SOL, linear device)}$$

$$\rho_s^2 \nabla_\perp \cdot \left\{ n \frac{d\nabla_\perp \phi}{dt} \right\} + \frac{2\rho_s C_s}{R} \frac{\partial n}{\partial y} = \frac{2C_s}{L_b} \frac{\rho_s}{\delta_b} n\phi \qquad \text{(close to separatrix)}$$

$$\rho_s^2 \nabla_\perp \cdot \left\{ n \frac{d\nabla_\perp \phi}{dt} \right\} + \frac{2\rho_s C_s}{R} \frac{\partial n}{\partial y} = -\frac{2\rho_s V_A}{L_b} n_{amb} \rho_s \nabla_\perp^2 \phi \text{ (large beta)}$$

- In some sense these equations are similar to the Boussinesq approximation of 2D Rayleigh-Taylor instability

$$d_t \nabla_\perp^2 \psi + g \frac{\partial T}{\partial y} = \mu \nabla_\perp^4 \psi, \qquad d_t T = 0,$$

- However, “dissipative” terms in bob equations are different from RT
- It brings structural stability of blobs and allow them to propagate on large distance as a coherent structure
- Drives due to parallel $\mathbf{E}\times\mathbf{B}$ shear and grad(Te) can result in blob radial convection with velocity closed to that observed in experiment

- Our studies of nonlinear structures driven by parallel $\mathbf{E}\times\mathbf{B}$ shear and $\nabla_{\perp}T_e$ drives pose more general question:

What is the role of long wavelength relatively slow but aperiodically growing modes?

- Often it is assumed that anomalous transport is described by diffusion with diffusion coefficient

$$D_{eff} \sim \gamma_{max} / k_{max}^2,$$

where γ_{max} is maximum value of the growth-rate and k_{max} is the wave number which corresponds to this growth-rate

- However, could it be that long wave-length aperiodically growing modes are responsible for non-diffusive (convective!?) transport of the structures (blobs/ELMs!?) with rather-stable scales $\sim k_*^{-1}$, such that $\mathbf{V}_E \cdot \mathbf{k} \sim \gamma$ and effective radial velocity

$$V_{eff} \sim \gamma_* / k_*$$

- Also, what is the role of high k modes and their interactions with these structures?

- Can high k modes alter convective transport? How?